Dyes and Pigments 93 (2012) 1519–1531

Contents lists available at ScienceDirect

Dyes and Pigments

journal homepage: www.elsevier.com/locate/dyepig

Review

Fine tuning of the one- and two-photon absorption properties of macrocyclic thiophene-based derivatives

Shuang Huang [a], Lu-Yi Zou [a], Ai-Min Ren [a,*], Yang Zhao [a], Xiao-Ting Liu [a], Jing-Fu Guo [b,*], Ji-Kang Feng [a]

[a] State Key Laboratory of Theoretical and Computational Chemistry, Institute of Theoretical Chemistry, Jilin University, Changchun 130023, People's Republic of China
[b] School of Physics, Northeast Normal University, Changchun 130021, People's Republic of China

ARTICLE INFO

Article history:
Received 19 April 2011
Received in revised form
5 July 2011
Accepted 6 July 2011
Available online 30 July 2011

Keywords:
Macrocyclic thiophene-based derivatives
One-photon absorption
Two-photon absorption
TPA cross-section
Electronic structure
ZINDO method

ABSTRACT

The geometrical and electronic structures, and one- and two-photon absorption properties of macrocyclic thiophenes possessing push-pull groups were investigated. It shows that $\lambda^{(1)}_{max}$s appear red-shift for the designed macrocycles with strong donor/acceptor (D/A) substituents, and the red-shifts enlarge as increasing the number of D/A pair. As a result, their two-photon absorption cross-section (δ_{max})s get larger, and the configurations with donor and acceptor location on the opposite site can result in larger δ_{max}, which is ascribed to the enlargement of the stronger intramolecular charge transfer (ICT) between D and A or the inside of the whole ring skeleton. Taking SII series of molecules as an example, the enlargement of the net charge change (ΔQ) is one factor for the increase of δ_{max}. Moreover, transition dipole moments (M_{0k} and M_{kn}) play important roles on the increase of δ_{max}. And the product of oscillator strengths ($f_{0k} \times f_{kn}$) is in proportion to δ_{max}.

1. Introduction

Materials with large nonlinear optical (NLO) responses are under intense attention due to their potential applications in chemistry, photonic, and biological imaging fields [1–3]. Two-photon absorption (TPA) as a nonlinear optical phenomenon has attracted increasing interest in recent years [4]. TPA properties of organic materials exhibit bright future for many advanced applications such as microfabrication [5,6], optical power limiting [7], three-dimensional optical data storage [5,8], and biophotonics [9,10], etc. Development of two-photon technology mainly depends on the successfully synthesizing of new material molecules possessing large TPA cross-section values at proper wavelengths. However, so far, the practical TPA materials remain limited. One of the most essential reasons is that the structure-property relationship is still unclear. Therefore, it is necessary to explore and investigate the relationship for new materials with large TPA cross-section and applicable in practice.

Thiophene as a conjugated structure unit has lower resonance energy compared with other conjugated electronic transmission, and it is more stable than that of the electronic transmission with oligomers [11,12]. Therefore, compounds with thiophene as conjugated bridge may concurrently have stronger two-photon excited fluorescence property and better stability [13]. In addition to many thiophene derivatives with linear and branched architectures [14], a number of novel macrocyclic molecules have attracted great attentions in recent years [15–17]. Our current focus is to assemble new molecular materials using π-conjugated unit of macrocycle as modular building block. If the macrocyclic systems are sufficiently large and stable, novel electronic properties and applied perspectives will occur.

A series of fully π-conjugated macrocyclic thiophene-based derivatives C[3T_DA]$_n$ ($n = 2$–5), whose main body consist of trithiophene and diacetylene units have been successfully synthesized and reported by Theodore Goodson III et al. [15]. It was suggested that π-conjugated macrocycle can be extended by increasing the number of the building blocks. Usually, compound with donor-π-acceptor (D–π–A type) has large TPA cross-section, however, when the π-electron bridge is macrocyclic thiophene different from the ordinary linear conjugation one, the TPA property of such kind of compound remains unclear. Our group had reported the part of investigation on one- and two-photon absorption properties of macrocyclic thiophenes (SII–SV shown in Fig. 1) and suggested that size of annular thiophene compounds is closely related to large TPA cross-section value and large static second order nonlinear optical susceptibility [18,19]. As we know,

* Corresponding authors.
E-mail address: aimin_ren@yahoo.com (A.-M. Ren).

0143-7208/$ – see front matter © 2011 Elsevier Ltd. All rights reserved.
doi:10.1016/j.dyepig.2011.07.003

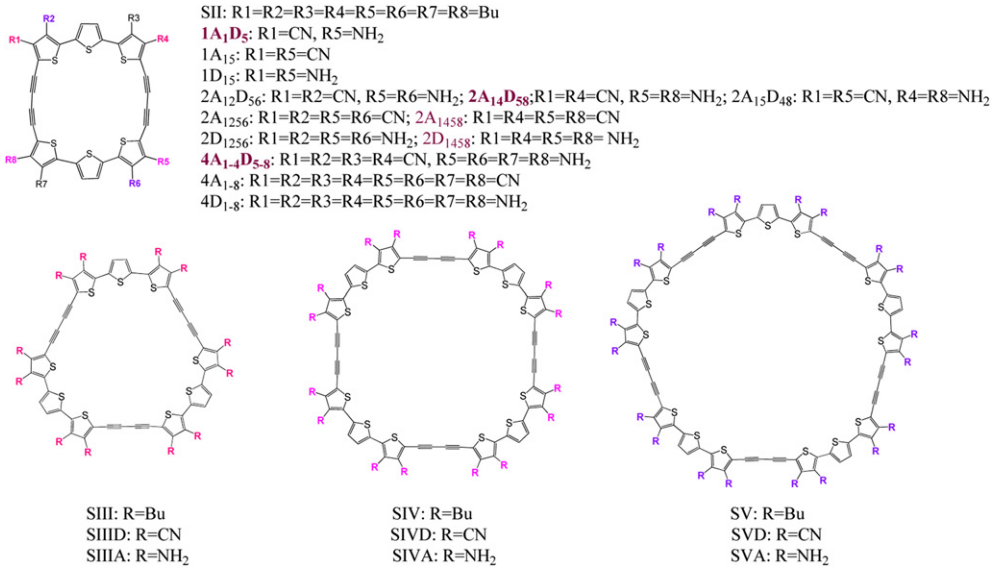

Fig. 1. Structures of the studied molecules.

induced effect of the substituent is essential to increase TPA response for the ordinary linear conjugated compounds [20]. So it is worth investigating how to tune and modify one- and two-photon absorption (OPA and TPA) properties through donor ($-NH_2$) or acceptor ($-CN$) group by means of different position setting and number of substituent for such macrocyclic thiophene-based derivatives. To achieve this purpose we have designed four series of molecules shown in Fig. 1. Their OPA and TPA properties were studied by using DFT and ZINDO program. The relationship between intramolecular charge transfer (ICT) and TPA cross-section (δ_{max}) of the studied molecules was identified by taking advantage of the TPA computation, the frontier molecular orbitals and the net

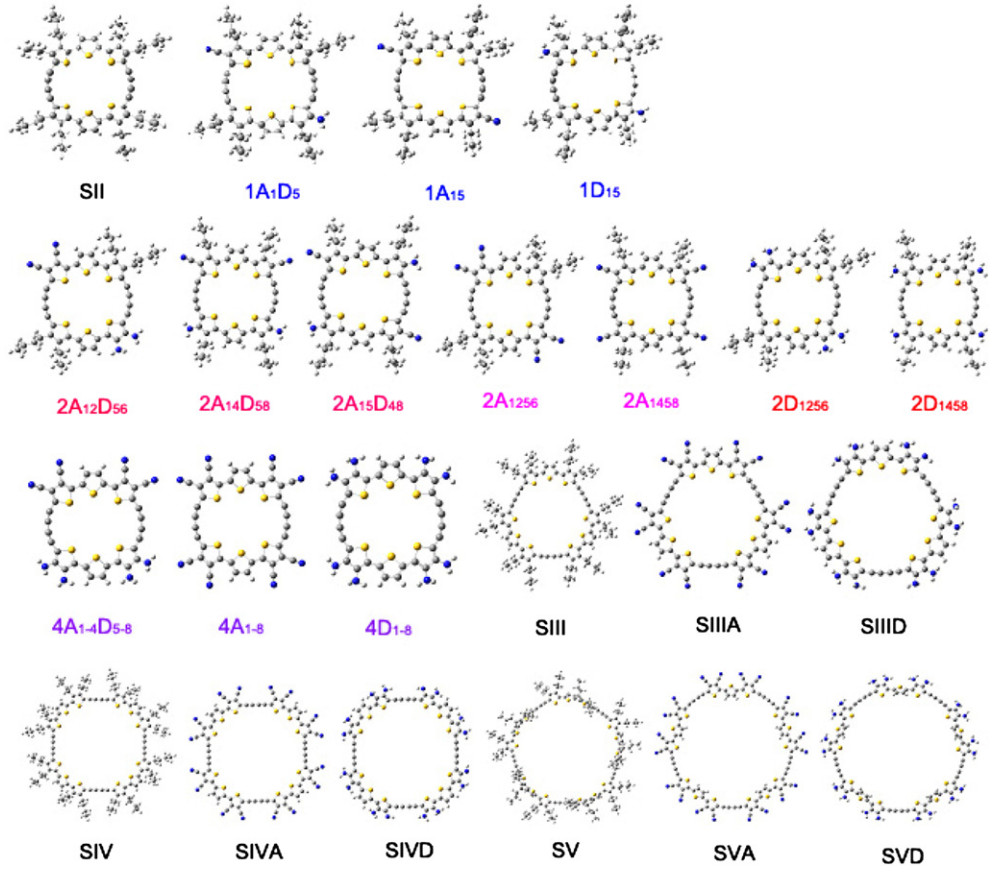

Fig. 2. The optimized structures of studied molecules in gas phase.

charge change (ΔQ). Moreover, the dependences of δ_{max} on the transition dipole moments (M_{0k} and M_{kn}), and the product of oscillator strengths (f_{0k} and f_{kn}) were investigated.

2. Theoretical methodology

In this work, MPWB95 functional [21,22] combined with the standard 6–31G (D) basis set was primarily adopted to calculate molecular equilibrium geometry in the Gaussian 03 program package [23]. MPWB95 functional arose in 2004, it is a novel functional compared with B3LYP. MPWB95 functional has made up the shortcomings of B3LYP functional, which is suitable for the systems with charge transfer, hydrogen bonds effect, π–π interaction, weak interaction, and has high accuracy for calculating dissociation energy of bond and enthalpy of formation. [21,22] For the series of macrocycle thiophenes, we have demonstrated this functional is more suitable for description its electron spectra than B3LYP in our previous paper [18,19].

And then, the property of electronic excited states was obtained by single and double electron excitation configuration interaction (SDCI) employing ZINDO program [24]. As well known that the original ZINDO algorithm (obtained by Zerner) has been adapted only to single-CI, but a double excitation configuration also needs to be considered for correct determination of the third-order polarizability (γ) and two-photon absorption spectrum. Thus, the double excitation configurations were added in ZINDO calculation and the CI-active spaces were restricted to five highest occupied and five lowest unoccupied π-orbitals [25]. Combining with the single-CI

Table 1
One-photon absorption properties calculated by ZINDO method.

Compound	$\lambda^{(1)}_{max}$/nm	f_{0k}	Transition nature			Compound	$\lambda^{(1)}_{max}$/nm	f_{0k}	Transition nature		
SII	409.4	0.963	$S_0 \rightarrow S_4$	H−1 → L	33.87%	$4A_{1-8}$	435.2	1.947	$S_0 \rightarrow S_4$	H → L+1	56.30%
				H → L + 2	29.33%					H−1 → L	34.84%
	392.5	1.649	$S_0 \rightarrow S_5$	H → L + 1	60.28%		428.6	1.200	$S_0 \rightarrow S_5$	H → L+2	42.66%
				H−2 → L	25.14%					H−2 → L	29.16%
	400[14–17]										
$1A_1D_5$	411.3	0.911	$S_0 \rightarrow S_3$	H−1 → L	26.67%	$4D_{1-8}$	414.8	0.921	$S_0 \rightarrow S_4$	H−1 → L	32.71%
				H−1 → L + 1	24.82%					H → L+2	30.70%
	393.7	1.129	$S_0 \rightarrow S_5$	H−2 → L	21.93%		398.7	1.782	$S_0 \rightarrow S_5$	H → L+1	57.90%
				H → L + 1	21.14%					H−2 → L	30.17%
				H → L + 2	19.61%						
$1A_{15}$	424.1	1.033	$S_0 \rightarrow S_4$	H → L+1	44.81%	SIII	421.4	2.392	$S_0 \rightarrow S_2$	H → L+1	37.06%
				H−2 → L	16.57%					H−1 → L	33.09%
	397.5	1.325	$S_0 \rightarrow S_5$	H−1 → L	51.53%		421.4	2.392	$S_0 \rightarrow S_3$	H → L+2	37.06%
				H → L+2	18.23%					H−2 → L	33.09%
							422[16,17]				
$1D_{15}$	411.1	1.004	$S_0 \rightarrow S_4$	H−1 → L	42.12%	SIIIA	464.3	2.583	$S_0 \rightarrow S_2$	H → L+1	42.83%
				H → L+2	25.50%					H−1 → L	33.37%
	390.8	1.266	$S_0 \rightarrow S_5$	H → L+1	69.22%		464.3	2.583	$S_0 \rightarrow S_3$	H → L+2	42.83%
										H−2 → L	33.37%
$2A_{12}D_{56}$	414.7	0.689	$S_0 \rightarrow S_4$	H−2 → L	20.47%	SIIID	441.6	2.181	$S_0 \rightarrow S_2$	H → L+1	35.30%
				H → L+2	19.85%					H−1 → L	34.25%
	404.4	0.804	$S_0 \rightarrow S_6$	H → L+1	22.67%		441.6	2.181	$S_0 \rightarrow S_3$	H → L+2	35.30%
				H → L+2	20.77%					H−2 → L	34.24%
$2A_{14}D_{58}$	432.0	1.132	$S_0 \rightarrow S_4$	H → L+1	40.70%	SIV	452.1	3.011	$S_0 \rightarrow S_2$	H → L+2	25.08%
				H−1 → L	29.33%		452.1	3.011	$S_0 \rightarrow S_3$	H → L+1	25.08%
	394.3	1.562	$S_0 \rightarrow S_5$	H → L+2	51.44%		420[16,17]				
				H−2 → L	33.67%						
$2A_{15}D_{48}$	419.1	1.173	$S_0 \rightarrow S_4$	H → L + 1	42.09%	SIVA	508.3	3.231	$S_0 \rightarrow S_2$	H → L + 1	28.05%
				H-1 → L	24.48%					H−2 → L	27.46%
	373.4	1.063	$S_0 \rightarrow S_8$	H−2 → L	43.69%		508.3	3.231	$S_0 \rightarrow S_3$	H → L+2	28.05%
				H → L + 2	22.46%					H−1 → L	27.46%
$2A_{1256}$	427.6	1.254	$S_0 \rightarrow S_4$	H → L + 1	64.94%	SIVD	462.5	2.889	$S_0 \rightarrow S_2$	H → L + 1	26.10%
	411.9	0.940	$S_0 \rightarrow S_5$	H−1 → L	25.65%					H−2 → L	22.84%
				H−2 → L	20.10%					H → L + 2	26.10%
							462.5	2.889	$S_0 \rightarrow S_3$	H−1 → L	22.84%
$2A_{1458}$	427.4	1.073	$S_0 \rightarrow S_4$	H → L+1	57.20%	SV	464.4	3.592	$S_0 \rightarrow S_2$	H → L+1	23.75%
				H−2 → L	15.87%					H−1 → L	23.06%
	401.8	1.232	$S_0 \rightarrow S_5$	H−1 → L	66.96%		464.4	3.592	$S_0 \rightarrow S_3$	H → L+2	23.75%
										H−2 → L	23.06%
							433[15–17]				
$2D_{1256}$	411.7	0.902	$S_0 \rightarrow S_4$	H−1 → L	31.26%	SVA	530.2	3.834	$S_0 \rightarrow S_2$	H → L+1	26.78%
				H → L + 2	25.08%					H−1 → L	25.46%
	392.5	1.608	$S_0 \rightarrow S_5$	H → L + 1	52.39%		530.2	3.834	$S_0 \rightarrow S_3$	H → L+2	26.78%
				H−2 → L	26.29%					H−2 → L	25.46%
$2D_{1458}$	419.4	0.742	$S_0 \rightarrow S_4$	H−1 → L	27.71%	SVD	500.2	3.611	$S_0 \rightarrow S_2$	H → L + 1	25.04%
				H → L + 2	19.68%					H−1 → L	24.29%
	396.9	1.150	$S_0 \rightarrow S_5$	H → L + 1	69.27%		500.2	3.611	$S_0 \rightarrow S_3$	H → L + 2	25.04%
										H−2 → L	24.29%
$4A_{1-4}D_{5-8}$	418.9	1.450	$S_0 \rightarrow S_6$	H → L + 2	64.23%						

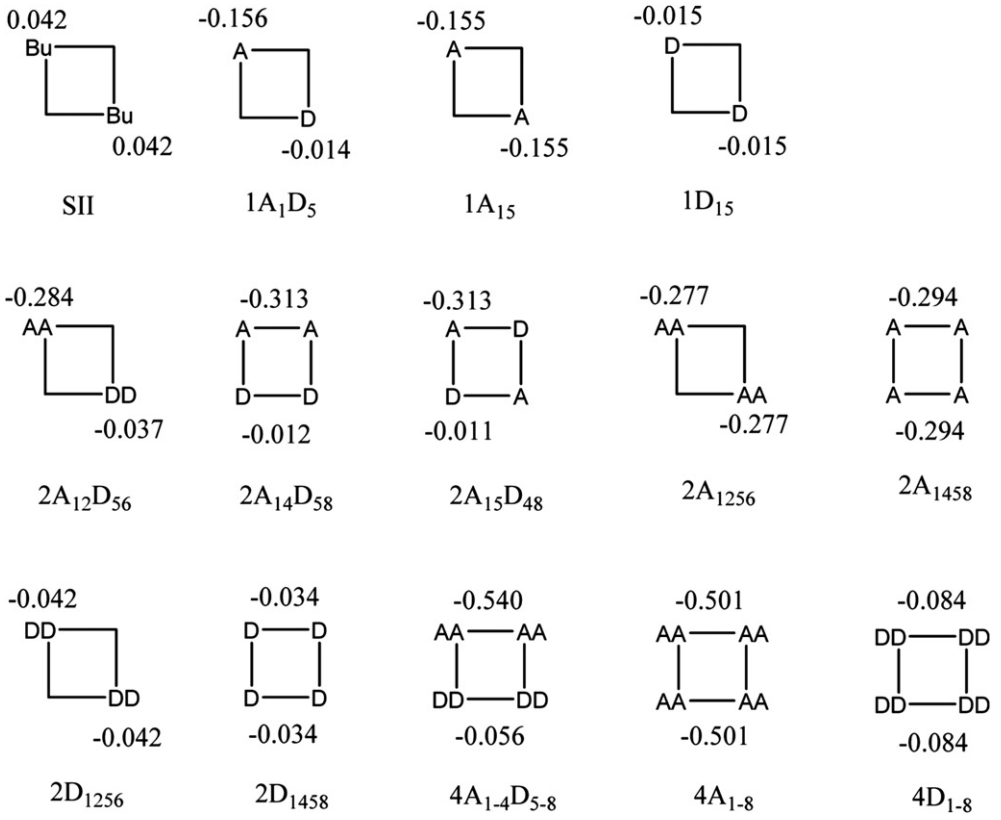

Fig. 3. The net charge (Q_0) of A/D substituents in SII series of molecules in ground state.

from 20 highest occupied orbitals and 20 lowest unoccupied orbitals, there are in all 826 configuration states in the CI calculation. Then, a program (FTRNLO) compiled by our group was adopted to calculate the second hyperpolarizability (γ) and the TPA cross-section (δ_{max}) according to following Eqs. (1) and (2).

The magnitude of the TPA efficiency of an organic molecule, at optical frequency $\omega/2\pi$, can be characterized by the TPA cross-section $\delta(\omega)$, which can be directly related to the imaginary part of the third-order polarizability $\gamma(-\omega; \omega, \omega, -\omega)$ [26], as shown in Eq. (1):

$$\delta(\omega) = \frac{3(\hbar\omega)^2}{2n^2c^2\varepsilon_0\hbar}L^4\mathrm{Im}[\gamma(-\omega;\omega,-\omega,\omega)] \quad (1)$$

where $\gamma(-\omega; \omega, \omega, -\omega)$ is the third-order polarizability; $\hbar\omega$ is the energy of incoming photons; c is the speed of light; ε_0 is the vacuum electric permittivity; n indicates the refractive index of the medium, and L corresponds to the local-field factor. During the calculation exhibited here, n and L are set to 1 due to isolated molecules in the vacuum.

The sum-over-states (SOS) expression that is applied to evaluate the components of the second hyperpolarizability ($\gamma_{\alpha\beta\gamma\delta}$), can be deduced using perturbation theory. Through considering a Taylor expansion of energy with respect to the applied field, the $\gamma_{\alpha\beta\gamma\delta}$ Cartesian components are given by references [27] and [28].

To compare the calculated δ value with the experimental value, the damping factor (Γ) of excited state K in the SOS expression is set to 0.14 eV in our work, which is found to be reasonable based on the comparison between the theoretical calculation and experimental TPA spectra. And the orientationally averaged (isotropic) value of γ is evaluated, which is defined as

$$\langle\gamma\rangle = \frac{1}{15}\sum_{i,j}\left(\gamma_{iijj}+\gamma_{ijij}+\gamma_{ijji}\right), \quad i,j = x,y,z \quad (2)$$

after $\langle\gamma\rangle$ is taken into Eq. (1), the TPA cross section δ is obtained.

Generally, the position and relative strength of the two-photon resonance are predicted using the following simplified form of the SOS expression as followed [29],

$$\delta \propto \frac{M_{0k}^2 M_{kn}^2}{(E_{0k}-E_{0n}/2)^2\Gamma} + \frac{M_{0n}^2\Delta\mu_{0n}^2}{(E_{0n}/2)^2\Gamma} \quad (3)$$

where M_{ij} is the transition dipole moment from the state i to j; E_{ij} is the corresponding excitation energy, the subscripts 0, k and n refer to the ground state S_0, the intermediate state S_k, and the TPA final

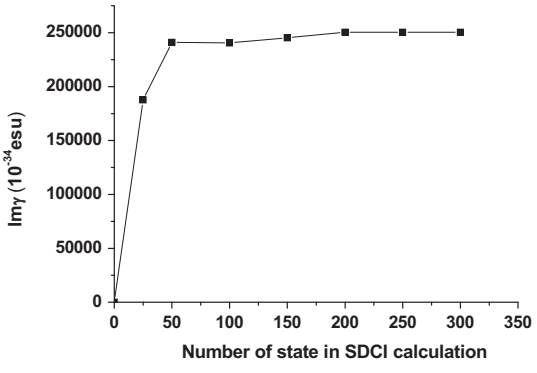

Fig. 4. Dependence of imaginary part of γ (Im γ) on state number for SV molecule.

state S_n, respectively; M_{0n} is the transition dipole moment from S_0 to S_n. $\Delta\mu_{0n}$ is the difference of dipole moment between S_0 to S_n.

In principle, any kind of self-consistent field molecular orbital procedure in combination with configuration interaction can be used to calculate the physical values according to the above expression.

3. Results and discussion

3.1. Molecular design and geometry optimization

To improve the polarization of macrocyclic thiophene derivatives, electron donor and acceptor were introduced to outer lateral

Table 2
Two-photon absorption properties of studied molecules.

Compound	$\lambda^{(2)}_{max}$/nm	Transition nature	Im γ /1×10^{-34} esu			δ_{max}/GM	Compound	$\lambda^{(2)}_{max}$/nm	Transition nature		Im γ /1×10^{-34} esu	δ_{max}/GM
SII	652.6	$S_0\rightarrow S_{14}$	H,H → L,L	14.91%	12009.4	465.2	$4A_{1-8}$	694.2	$S_0\rightarrow S_{14}$	H → L + 4	21.31%	19889.4	680.7
			H → L + 3	13.26%						H−1 → L + 2	14.32%		
										H,H → L,L	13.47%		
	741.5					181.0							
	760.6					143.7							
	760[15]					105[15]		594.4	$S_0\rightarrow S_{28}$	H → L+7	26.51%	30960.6	1445.6
	650.5[a]					372.2[a]				H−2 → L+5	10.66%		
	760.6[a]					110.5[a]		691.9[a]					668.5[a]
$1A_1D_5$	660.9	$S_0\rightarrow S_{14}$	H → L + 3	12.43%	13691.7	517.0	$4D_{1-8}$	669.5	$S_0\rightarrow S_{14}$	H → L+3	27.84%	13545.7	498.5
			H−1 → L + 2	11.11%						H−1 → L+1	11.48%		
										H,H → L,L	10.76%		
	658.8[a]					444.7[a]		642.4[a]					314.6[a]
$1A_{15}$	658.8	$S_0\rightarrow S_{14}$	H−5 → L	13.19%	12711.8	483.1	SIII	667.3	$S_0\rightarrow S_{13}$	H−3 → L	24.76%	53536.0	1983.1
			H,H → L,L	11.04%						H → L + 3	11.56%		
			H → L+4	10.85%									
			H−1 → L+1	10.01%				733.6					851.8
	746.9					237.2	SIIIA	665.2	$S_0\rightarrow S_{19}$	H → L + 5	27.14%	76661.6	2858.0
	660.9[a]					481.0[a]				H−2 → L + 3	11.09%		
$1D_{15}$	660.9	$S_0\rightarrow S_{13}$	H,H → L,L	15.70%	11933.2	450.6				H−1 → L + 4	11.09%		
	738.9					173.0		592.7	$S_0\rightarrow S_{33}$	H−1,H → L,L + 1	12.68%	196320.1	9219.1
	652.6[a]					345.6[a]				H−2,H → L,L + 2	12.68%		
								746.9					2364.6
							SIIID	676.0	$S_0\rightarrow S_{17}$	H,H → L,L	13.08%	40533.9	1462.9
								749.6					721.0
$2A_{12}D_{56}$	671.6	$S_0\rightarrow S_{14}$	H−1 → L+1	16.72%	14427.1	527.5	SIV	640.4	$S_0\rightarrow S_{21}$	H−4 → L	18.87%	96072.1	3863.7
			H−2 → L+2	13.98%						H → L+3	10.31%		
			H → L+4	12.38%				701.3					3616.6
	824.4					132.1		656.7[a]					3472.4[a]
	665.2[a]					489.4[a]							
$2A_{14}D_{58}$	665.2	$S_0\rightarrow S_{14}$	H,H → L,L	20.75%	16149.2	602.1	SIVA	689.6	$S_0\rightarrow S_{18}$	H,H → L,L	13.26%	186204.0	6459.0
	746.9					247.0		587.6	$S_0\rightarrow S_{50}$	H−3 → L+4	13.85%	548862.5	26219.7
	669.5[a]					500.7[a]							
$2A_{15}D_{48}$	671.6	$S_0\rightarrow S_{14}$	H,H → L,L	14.92%	15750.4	575.9		715.8					6351.6
			H−2 → L+1	14.44%				795.8					3559.4
			H-1 → L+2	12.16%				682.7[a]					6342.7[a]
	669.5[a]					499.6[a]							
$2A_{1256}$	669.5	$S_0\rightarrow S_{14}$	H−2 → L+2	15.27%	13212.5	486.2	SIVD	613.8	$S_0\rightarrow S_{24}$	H−3 → L	11.86%	93925.0	4112.3
			H → L	10.25%						H → L+3	10.05%		
	671.6[a]					493.2[a]		701.3					3018.2
$2A_{1458}$	667.3	$S_0\rightarrow S_{14}$	H → L+4	27.61%	15666.4	580.3		656.7[a]					4222.0[a]
	757.8					235.1							
	671.6[a]					557.8[a]							
$2D_{1256}$	656.7	$S_0\rightarrow S_{14}$	H → L+3	11.88%	11504.7	440.0	SV	669.5	$S_0\rightarrow S_{16}$	H−2 → L+1	15.80%	244471.2	8997.2
			H,H → L,L	11.50%						H−1 → L+2	15.80%		
			H → L+4	10.31%						H−4 → L+3	14.925		
										H−3 → L+4	14.92%		
	741.5					162.4							
	652.6[a]					376.8[a]							
$2D_{1458}$	658.8	$S_0\rightarrow S_{14}$	H,H → L,L	30.19%	13437.7	510.7		760.6					578.4
			H−1 → L+1	13.32%				760[15]					1470[15]
	744.2					232.0	SVA	648.5	$S_0\rightarrow S_{26}$	H,H → L,L	11.32%	181105.4	7104.1
	646.4[a]					296.1[a]		738.9	$S_0\rightarrow S_{18}$	H−4 → L	15.44%	324415.4	9801.3
$4A_{1-4}D_{5-8}$	691.9	$S_0\rightarrow S_{15}$	H−2 → L+2	42.75%	19807.6	682.5							
			H−1 → L+1	12.46%									
	603.0	$S_0\rightarrow S_{23}$	H−2,H → L,L	14.79%	35753.0	1621.6	SVD	687.3	$S_0\rightarrow S_{24}$	H−3 → L	16.17%	290679.7	10150.5
										H → L+4	11.31%		
	851.5					141.8							
	689.6[a]					655.3[a]		713.4	$S_0\rightarrow S_{15}$	H−2 → L+1	17.08%	315349.5	10221.0
										H−1 → L+2	17.08%		
										H−4 → L+4	14.77%		
										H−3 → L+3	14.77%		

[a] Calculated values for SII and SIV series of molecules with C_i symmetry.

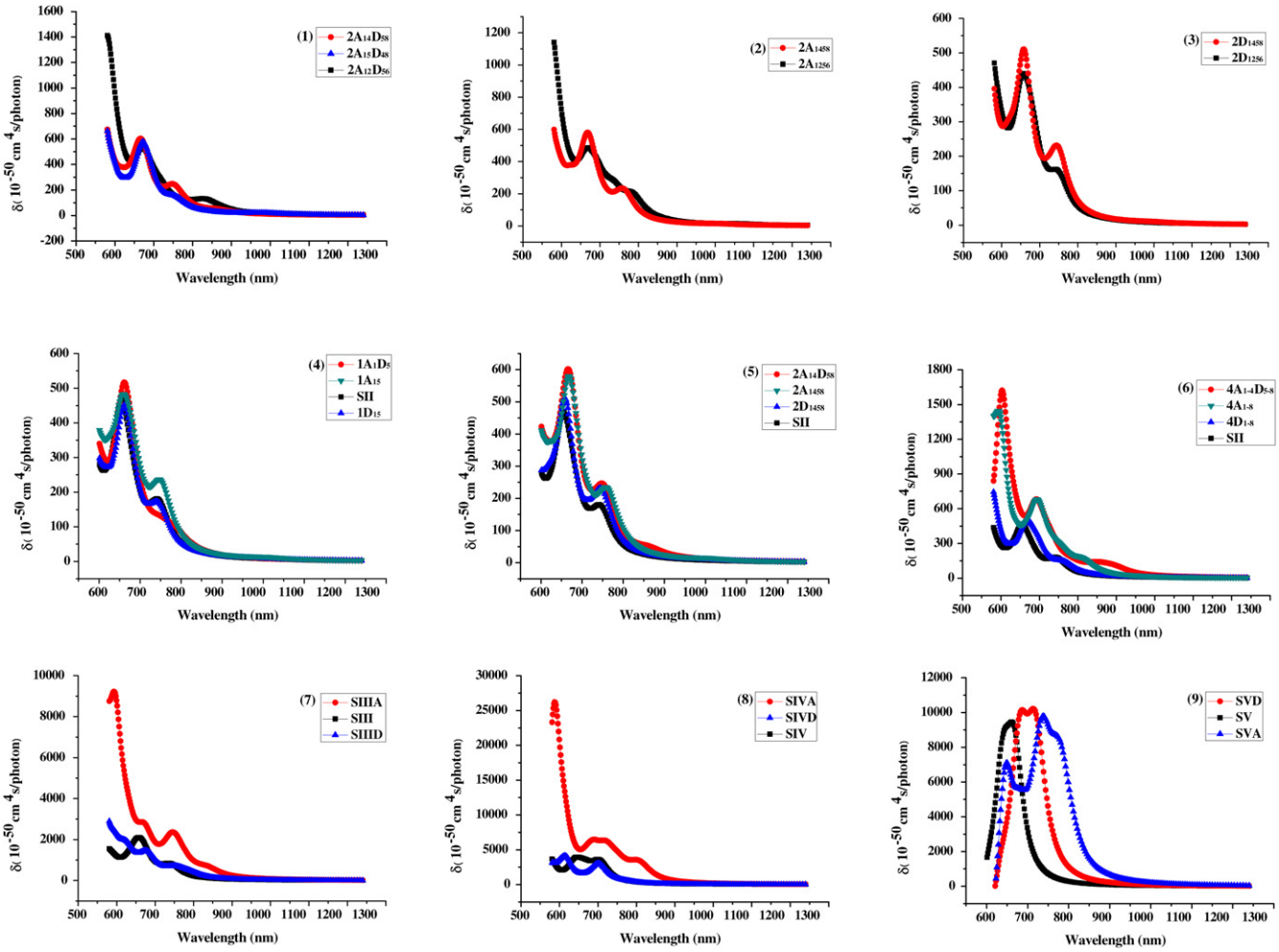

Fig. 5. Two-photon absorption spectra for studied molecules.

of the macrocycles to strengthen ICT. On the basis of the reported molecules C[3T_DA]$_n$ ($n = 2$–5) (named as SII–SV, here) [18,19], three types of macrocyclic thiophene-based compounds with D–π–A, A–π–A or D–π–D structure were designed by replacing butyl with electron donor (–NH_2) or acceptor (–CN). And the molecular structures are shown in Fig. 1. Firstly, SII series of molecules are chosen as an example to discuss the substitution effect of three kinds of designed molecules: i) molecules with one pair of electron donor or acceptor (D/A), $1A_1D_5$, $1A_{15}$, and $1D_{15}$, (where 1 stands for one pair of D/A, A represents acceptor, D denotes donor, and subscription 15 expresses position of substituent); ii) molecules with two pairs of D/A, $2A_{12}D_{56}$, $2A_{14}D_{58}$, $2A_{15}D_{48}$, $2A_{1256}$, $2A_{1458}$, $2D_{1256}$, and $2D_{1458}$; iii) ones with four pairs of D/A, $4A_{1-4}D_{5-8}$, $4A_{1-8}$ and $4D_{1-8}$. And then the different substituted positions for molecules with two pairs of D/A were considered specially. Secondly, when all butyls of SIII–SV molecules were substituted by –CN or –NH_2, molecules SIIIA and SIIID, SIVA and SIVD, and SVA and SVD were formed and discussed, respectively.

In order to study the OPA and TPA regularities of these macrocyclic thiophene-based compounds, all the structures with C_n symmetry were investigated, and some other isomers such as SII and SIV with C_i symmetry [30,31] were also considered herein. All the geometrical structures of these molecules were optimized using MPWB95 functional with 6–31G (D) basis set. It can be seen from Fig. 2 that the main body frameworks of all the optimized designed molecules are similar to the basic molecules SII–SV, respectively, which structure features are that the trithiophene moieties of each molecule slightly distort and are not in a plane and the arrangements of the middle thiophenes turn upwards and other two downwards. While, the donor and acceptor groups are almost situated at the same side of the macrocyclic surface. Moreover, frequency calculations were carried out, and suggested that all the geometries are stable without imaginary frequency.

3.2. One-photon absorption property

Based on the optimized geometries obtained by MPWB95/6–31G (D) method, their OPA properties have been calculated by ZINDO method, in which π–π overlap weighting factor was rectified as 0.51. The calculated results are presented in Table 1 and show that the absorption spectra of all studied molecules have more than one intense absorption peak, except molecule $4A_{1-4}D_{5-8}$. On one hand, compared with molecule SII, the $\lambda^{(1)}_{max}$s of all designed SII series of molecules (i.e. molecule SII is not included) are red-shifted, except molecules $1D_{15}$ and $4D_{1-8}$ are slightly blue-shifted. No matter which type of substitution (D–A, A–A or D–D), all the shifts of $\lambda^{(1)}_{max}$ get larger under increasing the pair number of substituent, and the maximum shift reaches to 42.7 nm. Whereas the change of $\lambda^{(1)}_{max}$s is slight for the molecules with two pairs of D/A, but corresponding oscillator strengths (f_{0k}) is changed largely (from 0.804 to 1.608). The analysis of transition

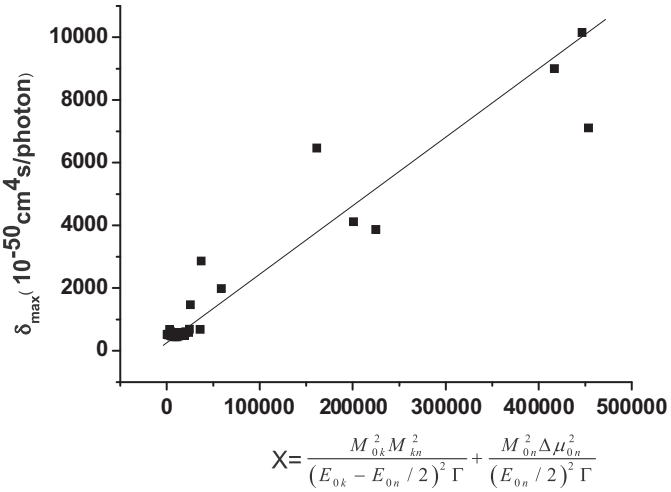

Fig. 6. The relationship between δ_{max} and X of studied molecules.

nature suggested that all the maximum OPA peaks are dominated by the transitions from HOMO−1 to LUMO, HOMO−2 to LUMO, HOMO to LUMO + 1 and HOMO to LUMO + 2. On the other hand, for SIII-SV series of molecules, the $\lambda^{(1)}_{max}$s of the designed molecules (SIIIA, SIIID, SIVA, SIVD, SVA, SVD) red shift by 10.4–65.8 nm. The f_{0k} of them are larger or smaller than that of the basic molecules SIII, SIV and SV, respectively, but both $\lambda^{(1)}_{max}$ and f_{0k} increase with the enlargement of the annular size. Their maximum OPA peaks are constructed by two degenerate excited states mixed with HOMO to LUMO + 1 or HOMO−1 to LUMO, and HOMO to LUMO + 2 or HOMO−2 to LUMO transitions. In a word, both increasing the number of D/A pair and enlarging the ring size can make $\lambda^{(1)}_{max}$ enlarge. In addition, all the values of $\lambda^{(1)}_{max}$ and f_{0k} for molecules with C_i symmetry are slightly smaller than that with C_n symmetry, respectively, but the increase trend with enlarging the ring size is the same as that for C_n symmetry.

Moreover, the OPA properties of SII series of molecules were further analyzed by net charge (Q_0) of the related substituents. As shown in Fig. 3, regarding to the three types of D–A, A–A and D–D molecules, the absolute value of Q_0 increases with increasing the number of D/A pair, and are all larger than that of SII molecule, and f_{0k} increases too (seen in Table 1), but the change of $\lambda^{(1)}_{max}$ is slight. It is known that dipole moment is equal to the product of charge and displacement. As all the added groups of D/A locate on the diagonal position, namely, the displacement between D–A, A–A or D–D and center is nearly the same, it can be deduced that the changing rule of dipole moment is the same as that of net charge (Q_0), that is, the oscillator strength (f_{0k}) enlarges as dipole moment increases. However, the origin of the enlargement for f_{0k} value is due to the presence of stronger D/A substituents.

3.3. Two-photon absorption property

Base on Eqs. (2), (3) and three-state approximation, the kth and the nth excited states with the largest transition moment M_{0k} and M_{kn} were selected as the intermediate state and the final state during TPA process, respectively. Thus the position of the maximum TPA peak ($\lambda^{(2)}_{max}$) were obtained in terms of Eqs. (1) and (2), the third-order optical susceptibility ($\langle\gamma\rangle$) and the TPA cross-section (δ_{max}) were calculated by ZINDO-SOS method. As well known, SOS expression is concerned with the truncation of sum terms, so the dependence of imaginary part of γ (Im γ) on number of excited state was analyzed. The result of the biggest molecule SV indicated that the Im γ converged before 300 states (Fig. 4). Thus 300 states are sufficient for the calculation here. And then, $\lambda^{(2)}_{max}$, Im γ, δ_{max}, and corresponding transition nature were collected and listed in Table 2.

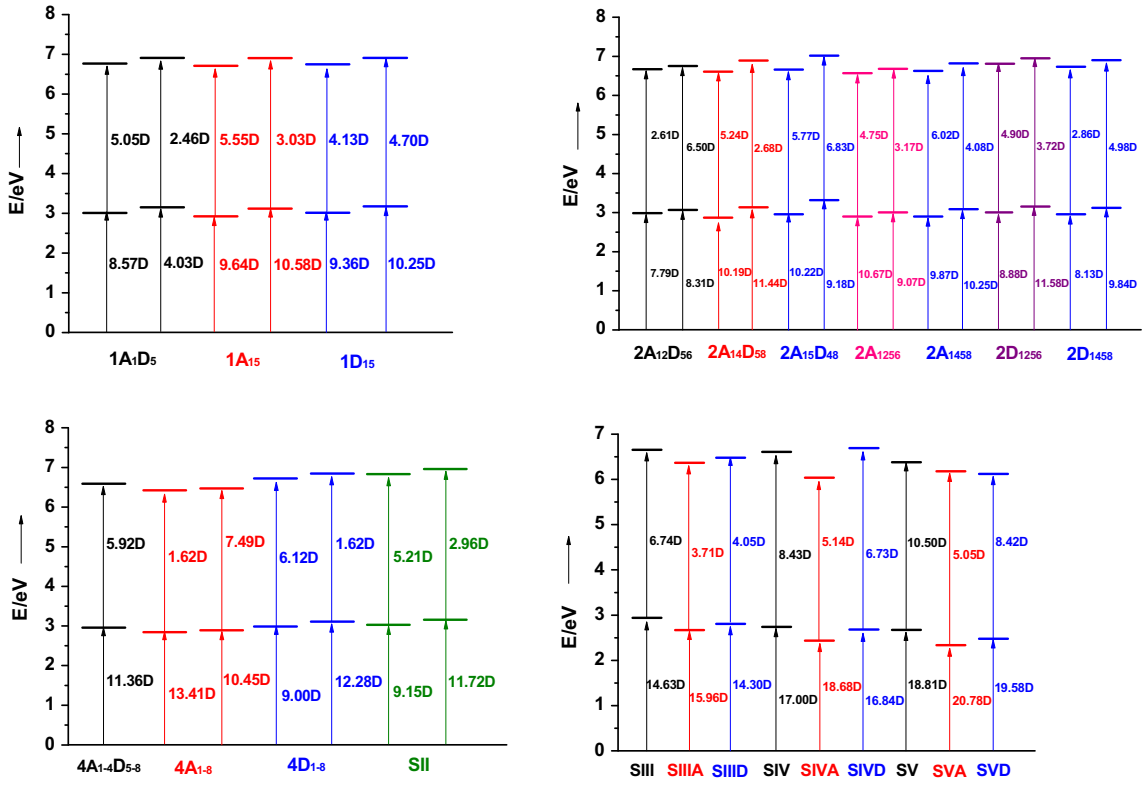

Fig. 7. Scheme of the calculated energy levels and the transition dipole moments (in Debyes).

Table 3
Some parameters of studied molecules calculated in TPA process.

Compound	Transition	$\Delta\mu_{0n}$	f_{kn}	$f_{0k} \times f_{kn}$	Compound	Transition	$\Delta\mu_{0n}$	f_{kn}	$f_{0k} \times f_{kn}$
SII	$S_0 \rightarrow S_4 \rightarrow S_{14}$	−0.019	0.080	0.077	$4A_{1-8}$	$S_0 \rightarrow S_4 \rightarrow S_{14}$	0.034	0.007	0.014
	$S_0 \rightarrow S_5 \rightarrow S_{14}$		0.021	0.035		$S_0 \rightarrow S_5 \rightarrow S_{14}$		0.146	0.175
$1A_1D_5$	$S_0 \rightarrow S_3 \rightarrow S_{14}$	4.294	0.072	0.066	$4D_{1-8}$	$S_0 \rightarrow S_4 \rightarrow S_{14}$	−0.031	0.106	0.098
	$S_0 \rightarrow S_5 \rightarrow S_{14}$		0.014	0.016		$S_0 \rightarrow S_5 \rightarrow S_{14}$		0.006	0.011
$1A_{15}$	$S_0 \rightarrow S_4 \rightarrow S_{14}$	0.074	0.101	0.104	SIII	$S_0 \rightarrow S_2 \rightarrow S_{13}$	0.220	0.133	0.318
	$S_0 \rightarrow S_5 \rightarrow S_{14}$		0.023	0.030		$S_0 \rightarrow S_3 \rightarrow S_{13}$		0.132	0.316
$1D_{15}$	$S_0 \rightarrow S_4 \rightarrow S_{13}$	−0.053	0.047	0.047	SIIIA	$S_0 \rightarrow S_2 \rightarrow S_{19}$	0.025	0.054	0.139
	$S_0 \rightarrow S_5 \rightarrow S_{13}$		0.047	0.060		$S_0 \rightarrow S_3 \rightarrow S_{19}$		0.054	0.139
$2A_{12}D_{56}$	$S_0 \rightarrow S_4 \rightarrow S_{14}$	−1.294	0.018	0.012	SIIID	$S_0 \rightarrow S_2 \rightarrow S_{17}$	0.181	0.054	0.118
	$S_0 \rightarrow S_6 \rightarrow S_{14}$		0.098	0.079		$S_0 \rightarrow S_3 \rightarrow S_{17}$		0.054	0.118
$2A_{14}D_{58}$	$S_0 \rightarrow S_4 \rightarrow S_{14}$	0.840	0.091	0.103	SIV	$S_0 \rightarrow S_2 \rightarrow S_{21}$	−0.132	0.304	0.915
	$S_0 \rightarrow S_5 \rightarrow S_{14}$		0.016	0.025		$S_0 \rightarrow S_3 \rightarrow S_{21}$		0.304	0.915
$2A_{15}D_{48}$	$S_0 \rightarrow S_4 \rightarrow S_{14}$	0.050	0.094	0.110	SIVA	$S_0 \rightarrow S_2 \rightarrow S_{18}$	−0.007	0.116	0.375
	$S_0 \rightarrow S_8 \rightarrow S_{14}$		0.067	0.071		$S_0 \rightarrow S_3 \rightarrow S_{18}$		0.116	0.375
$2A_{1256}$	$S_0 \rightarrow S_4 \rightarrow S_{14}$	−0.003	0.066	0.083	SIVD	$S_0 \rightarrow S_2 \rightarrow S_{24}$	0.063	0.229	0.662
	$S_0 \rightarrow S_5 \rightarrow S_{14}$		0.025	0.024		$S_0 \rightarrow S_3 \rightarrow S_{24}$		0.229	0.662
$2A_{1458}$	$S_0 \rightarrow S_4 \rightarrow S_{14}$	0.086	0.114	0.122	SV	$S_0 \rightarrow S_2 \rightarrow S_{16}$	0.449	0.434	1.559
	$S_0 \rightarrow S_5 \rightarrow S_{14}$		0.041	0.050		$S_0 \rightarrow S_3 \rightarrow S_{16}$		0.434	1.559
$2D_{1256}$	$S_0 \rightarrow S_4 \rightarrow S_{14}$	−0.037	0.071	0.064	SVA	$S_0 \rightarrow S_2 \rightarrow S_{26}$	0.757	0.146	0.560
	$S_0 \rightarrow S_5 \rightarrow S_{14}$		0.033	0.053		$S_0 \rightarrow S_3 \rightarrow S_{26}$		0.146	0.560
$2D_{1458}$	$S_0 \rightarrow S_4 \rightarrow S_{14}$	0.018	0.026	0.019	SVD	$S_0 \rightarrow S_2 \rightarrow S_{24}$	0.338	0.312	1.127
	$S_0 \rightarrow S_5 \rightarrow S_{14}$		0.061	0.070		$S_0 \rightarrow S_3 \rightarrow S_{24}$		0.312	1.127
$4A_{1-4}D_{5-8}$	$S_0 \rightarrow S_6 \rightarrow S_{15}$	−1.252	0.089	0.129					

3.3.1. Molecular structure and TPA peak

Since the TPA wavelength in near infrared region is useful in practice [32], and the TPA cross-section of molecules SII and SV were measured at 760 nm in experiment, thus, TPA peaks between the wavelength range of 580 and 1240 nm were calculated by point scanning, and the results were plotted in Fig. 5. The range of $\lambda^{(2)}_{max}$ for all the studied compounds is from 587.6 nm to 851.5 nm, a stronger TPA peak appears at 660 nm or so, and for molecules $4A_{1-4}D_{5-8}$, $4A_{1-8}$, SIIIA and SIVA have a much stronger one around 600 nm besides, which are assigned to the higher state transitions (i.e. $S_0 \rightarrow S_{23}$, $S_0 \rightarrow S_{28}$, $S_0 \rightarrow S_{33}$ and $S_0 \rightarrow S_{50}$, respectively) (shown in Table 2). In addition, most of molecules have secondary peak between 700 and 760 nm. Moreover, the maximum TPA peak $\lambda^{(2)}_{max}$ is red-shifted with increasing the number of trithiophene and diacetylene unit in the molecular skeleton.

3.3.2. Molecular structure and TPA cross-section

In combining with Table 2 and Fig. 5, TPA cross-sections of all studied molecules were analyzed in detail. On one hand, different substituted position is taken into the specific consideration for molecules with two pairs of D/A. As can be seen from Fig. 5(1) that $2A_{14}D_{58}$ with two electron donors and two acceptors located on the same side of the molecule, respectively, shows the largest δ_{max} compared with other two configurations ($2A_{12}D_{56}$ and $2A_{15}D_{48}$). This is ascribed to its strong ICT from electron donors to acceptors at the two ends of molecule. And that $2A_{1458}$ and $2D_{1458}$ possess larger δ_{max} values (seen in Fig. 5(2) and (3)) is attributed to the strong ICT between the whole ring skeletons and the substituents. Therefore, it was concluded that 1,4,5,8-positions of SII series of molecules have significant effect on TPA cross-section (δ_{max}). On the other hand, the push-pull property and the number of D/A pair in a molecule have also effect on δ_{max}. It can be known from Fig. 5(4)–(6) that the δ_{max} of $1A_1D_5$ and $1A_{15}$ are close, and larger than that of $1D_{15}$, and that of $2A_{14}D_{58}$ is similar to $2A_{1458}$ and larger than $2D_{1458}$, as well, that of $4A_{1-4}D_{5-8}$ is near to $4A_{1-8}$ and larger than $4D_{1-8}$. Therefore, the δ_{max} values increase as butyl is substituted by D–A or A–A, and the δ_{max} values for the D–D type are close to SII. And when butyl is substituted by the same type of donor or acceptor groups (D–A, A–A or D–D), all the δ_{max}s increase with increasing the number of D/A pair. In a word, δ_{max} can be effectively enlarged by increasing the number of D/A pair or introducing D–A or A–A substituents or as donor or acceptor substituted at the opposite site (14 vs 58, here).

The same as SII series of molecules, δ_{max} values of SIIIA, SIVA and SVA are larger than that of SIII, SIV and SV, respectively, but SIIID, SIVD and SVD are similar to SIII, SIV and SV, respectively (Fig. 5(7)–(9)). Therefore, replacing butyls with strong D–A or A–A can effectively enlarge the value of TPA cross-section. It is resulted from stronger ICT among diacetylene moieties, thiophene parts of

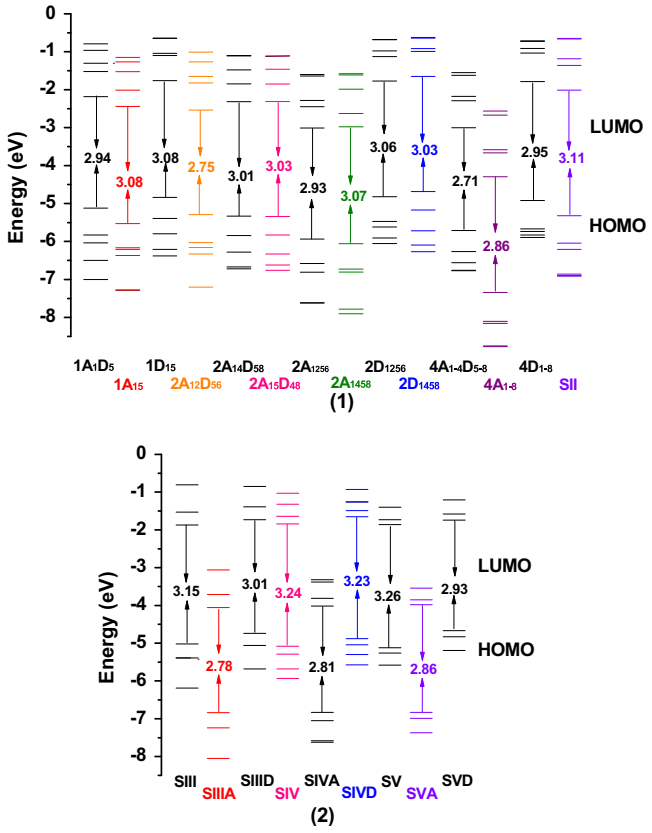

Fig. 8. MPWB95/6–31G (D) predicted molecular orbital energy diagrams.

the whole ring skeleton and the substituents. Moreover, the stronger the ability of the accepting or donating substituent is, the more obvious the ICT in molecular framework is. In short, the number, the position and push-pull property of D/A for a molecule are essentially significant for the enlargement of TPA cross-section. So changing the substituents of macrocyclic thiophene compounds can remarkably tune the value of TPA cross-section.

Furthermore, TPA wavelengths and cross-sections of SII and SIV series of molecules with C_i symmetry are also calculated and listed in Table 2. The results show maximum TPA peaks $\lambda^{(2)}_{max}$ are similar to that with C_n symmetry, and δ_{max} are slightly smaller than ones with C_n symmetry, however, both C_i and C_n isomers show the same trend for δ_{max}. It was concluded that, firstly, for SII series of molecules: i) Regarding to the two pairs of D/A substitutions, 1,4,5,8-substituted configurations have larger δ_{max} values; ii) The δ_{max} values of D–A and A–A types of compounds are nearly equal and larger than that of D–D, and the δ_{max} values of molecules with D–D type are similar to that of SII with butyls substituted; iii) Under the same type of substitution (D–A, A–A or D–D), all the δ_{max}s increase with increasing the number of D/A pair. Secondly, for SIV series of molecules, the δ_{max} of SIVA is larger than that of SIV and SIVD. In a word, the conclusion after considering C_i symmetry remains the same as those mentioned above, i.e. adding more and stronger push–pull, pull–pull substituents on marcocyclic thiophenes will significantly increase their TPA cross-section values.

In the SOS model, if only three important states, i.e. ground state, charge transfer state and TPA final state are considered, TPA cross-section can reduce to three states expression $X = (M^2_{0k}M^2_{kn})/((E_{0k} - E_{0n}/2)^2\Gamma) + (M^2_{0n}\Delta\mu^2_{0n})/((E_{0n}/2)^2\Gamma)$. The relationship between δ_{max} and X during the TPA process is depicted

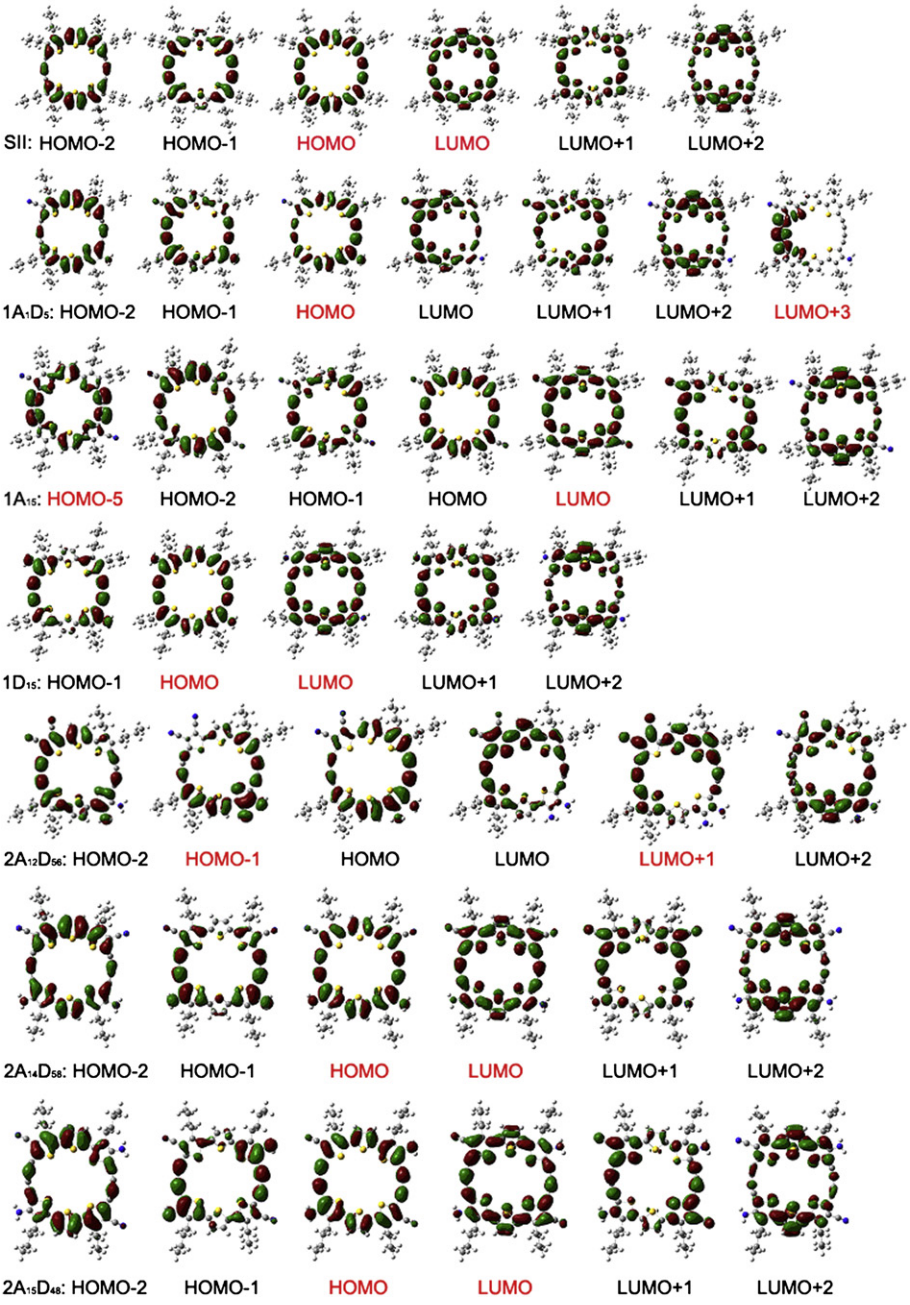

Fig. 9. Contour surfaces of the frontier orbitals relevant to OPA and TPA for studied molecules.

in Fig. 6, it shows an approximate proportional relationship between δ_{max} and X. And it indicates that X values of the studied molecules are largely in agreement with the change of their δ_{max}, so X can predict the changing trend of δ_{max} in general. Therefore, the transition dipole moments (M_{0k} and M_{kn}) are important factors influencing on the TPA cross-section in terms of the expression X. As illustrated in Fig. 7, M_{0k} values of D–A and A–A types of molecules are bigger, and have played important role in their δ_{max}. It can be seen from Table 3 that the difference of dipole moments between ground state and excited state ($\Delta\mu_{0n}$) of the molecules with D–A type of substitutions are bigger than that of other two types of molecules with A–A and D–D substituted, so it may lead to their larger δ_{max}. In short, besides δ_{max} values are affected by M_{0n} and M_{kn}, other factors also have some contributions to the increase of δ_{max}.

As mentioned above that f_{0k} (from ground state to intermediate state) increases with increasing the number of D/A pair for SII series of molecules, and enlarges as extending the ring size (Table 1). While the values of f_{kn} (from intermediate state to final state) have the similar change (Table 3). So it is proposed that there is proportional relationship between δ_{max} and $f_{0k} \times f_{kn}$. Therefore, oscillator strength can indirectly influence on the TPA cross-section.

3.4. Electronic structure and intramolecular charge transfer (ICT)

It will be useful to confirm the HOMO (the highest occupied orbital) and LUMO (the lowest unoccupied orbital) of molecules since the relative ordering of the occupied and virtual orbitals provides a reasonable qualitative indication of the excitation

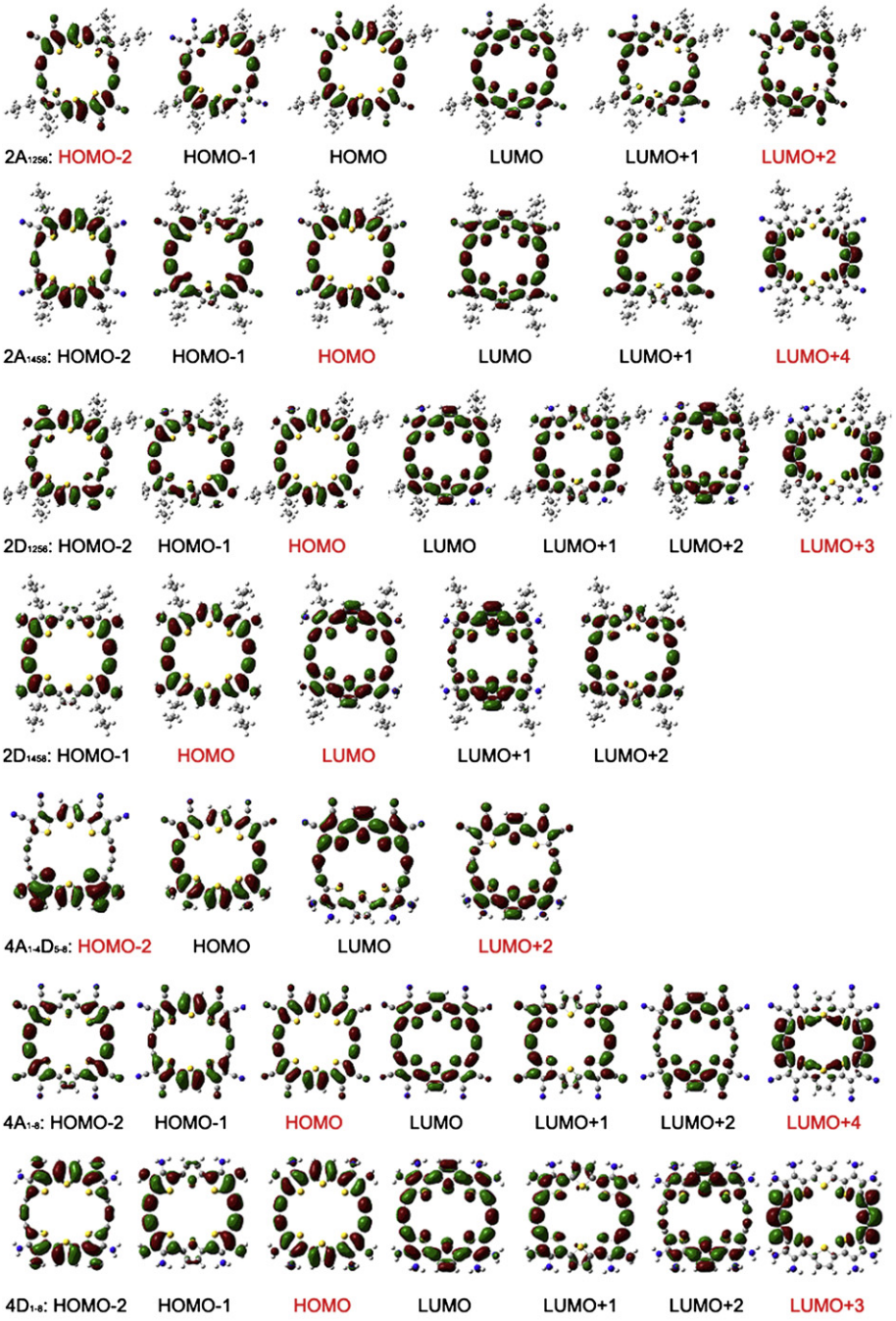

Fig. 9. (*continued*).

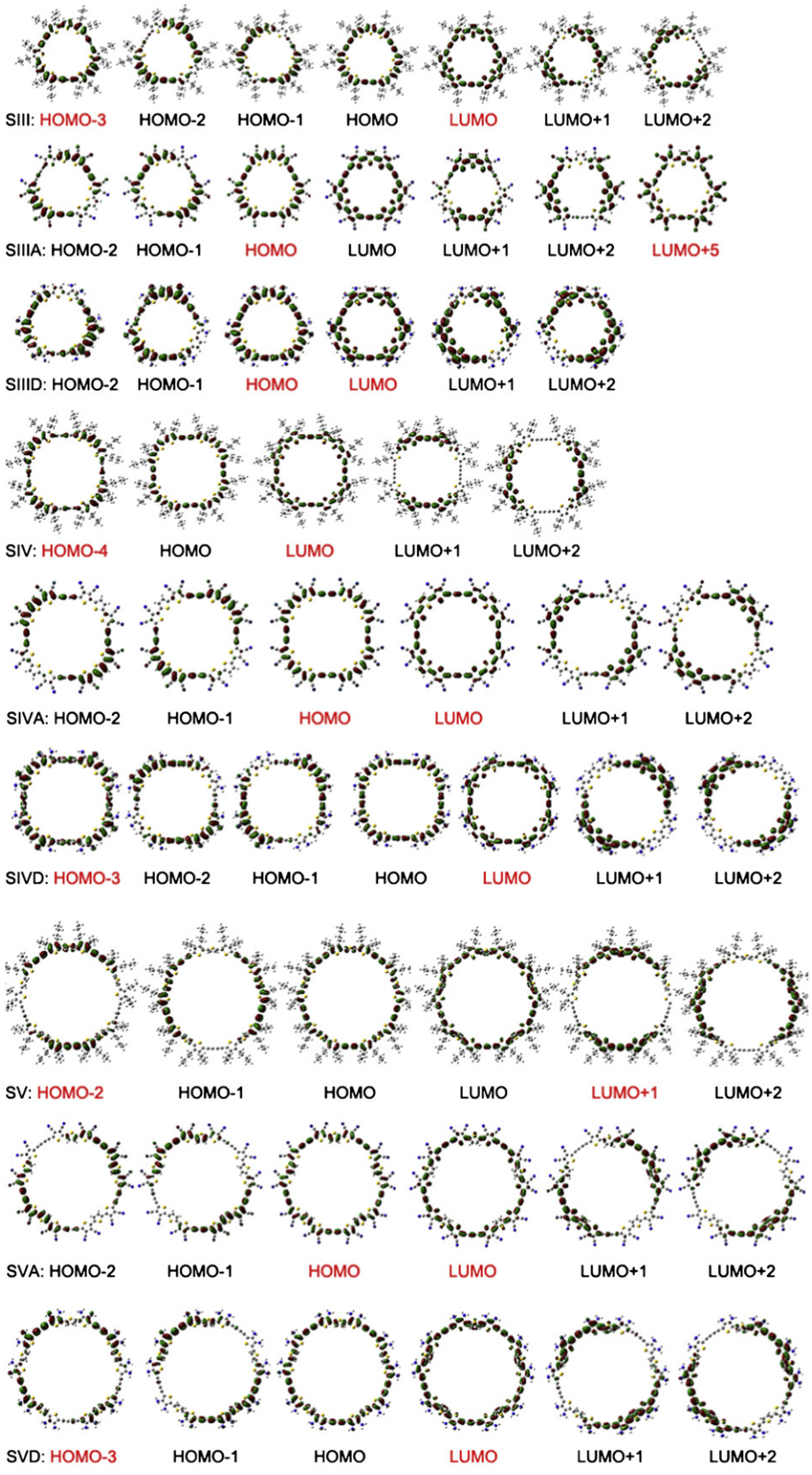

Fig. 9. (*continued*).

properties [12]. Therefore, HOMOs and LUMOs of the studied molecules are plotted in Fig. 8. For SII series of molecules, the ΔE_{H-L}s (energy gap between HOMO and LUMO) of new designed molecules (D–A, A–A and D–D) are all smaller than that of SII molecule, and ΔE_{H-L}s of D–A type of compounds are smaller than ones with A–A and D–D substituted. And HOMOs, LUMOs and ΔE_{H-L}s of SIIIA, SIVA and SVA are all smaller than that of the corresponding donor substituted and butyl ones, respectively. Namely, the energy gap of the compound with strong push–pull substituent is always smaller than those with weak push–pull group and unsubstituted one. In summary, the changing trend of ΔE_{H-L} is opposite to that of δ_{max}. The decrease of dynamic stability can lead to great electron transition probability, so that larger δ_{max} will be produced.

As is well known that the molecular orbital is closely related to electronic spectrum, thus contour plot of molecular frontier orbitals for studied molecules were shown in Fig. 9. The analysis of transition natures corresponding to every important excitation reveals that the electron clouds of SII molecule, and the series of SIII, SIV and SV molecules locate on the big ring skeleton and transfer among the parts in the whole skeleton, but none on the ambient butyl. However, the charge transfers of SII series of molecules with D–A and A–A types of substitutions are different from ones with D–D. The electron clouds of D–A and A–A types of compounds mostly locate on –CN, and that of D–D type concentrate in the macrocyclic skeleton. Additionally, the distributions of electron clouds strengthen as the number of D/A pair increases. It prefigures that the strength of ICT will enhance as increasing the number of D/A pair.

Since the NLO response is correlated to ICT during the excitation, in order to better understand the charge transfer in the TPA process and what group plays critical role on the TPA property, SII series of molecules were taken as an example to discuss the net charge change ($\Delta Q = Q_n - Q_0$) in the substituent and the ring skeleton. The calculated values of Mulliken charge of every part were listed in Table 4. Combing with the distribution of net charge in ground state (Q_0) (Fig. 3), it was concluded that Q_0 increases as the number of D/A pair increases, irrespective of the type of substitution (D–A, A–A or D–D). While the ΔQ_1 (ΔQ of substituent in Table 4) of molecules with two pairs of D/A, substituted at 1,4,5,8–positions ($2A_{14}D_{58}$, $2A_{1458}$ and $2D_{1458}$) are bigger, and it may lead to their larger ICT and δ_{max}. In addition, no matter how many D/A pairs are included, the Q_0 of D–A and A–A are similar and larger than that of D–D type, and ΔQ_1 has the same changing trend, which interprets the corresponding variety of δ_{max}. Moreover, the larger negative charges (ΔQ_1) for acceptor (–CN) substituent have explained the distribution of electron clouds about D–A and A–A types of compounds mostly location on –CN as mentioned above. To sum up, all the ΔQ_1 of the designed molecules enlarge no matter donor or acceptor replaces the butyl. The values of ΔQ_1 obviously describe the stronger push electron property of $-NH_2$ and pull electron property of –CN in a molecule and the substituents contribute to redistribution of the whole molecule. Of course, the ΔQ_2 (ΔQ of ring skeleton) of diacetylene and thiophene moieties (lateral and middle) in the ring skeleton have also well characterized the charge transfer. For example, the larger ΔQ_2 of SII, $1D_{15}$, $2D_{1458}$ and $4D_{1-8}$ have confirmed the more distribution of electron clouds in the ring skeleton. So that ICT among each part of the studied molecules are important for the increase of TPA cross-section value.

Table 4
The net charge change of substituent and ring skeleton in SII series of molecules.

Compound	ΔQ of substituent (ΔQ_1)		ΔQ of ring skeleton (ΔQ_2)		
	A (or up side)	D (or down side)	–C≡C–C≡C–	Lateral thiophene	Middle thiophene
SII	0.001 (1Bu) 0.002 (2Bu) 0.004 (4Bu)	0.001 (1Bu) 0.002 (2Bu) 0.004 (4Bu)	0.088	−0.127	0.031
$1A_1D_5$	−0.020	0.008	0.076	−0.098	0.027
$1A_{15}$	−0.023	−0.023	−0.017	−0.030	0.080
$1D_{15}$	0.007	0.007	0.091	−0.092	−0.019
$2A_{12}D_{56}$	−0.020	0.009	0.070	−0.099	0.035
$2A_{14}D_{58}$	−0.028	0.027	0.086	−0.129	0.041
$2A_{15}D_{48}$	−0.030	0.025	0.053	−0.099	0.047
$2A_{1256}$	−0.010	−0.010	0.049	−0.089	0.052
$2A_{1458}$	−0.024	−0.024	0.020	−0.001	0.021
$2D_{1256}$	0.007	0.007	0.098	−0.131	0.013
$2D_{1458}$	0.023	0.023	0.159	−0.072	−0.132
$4A_{1-4}D_{5-8}$	−0.023	0.022	0.065	−0.099	0.035
$4A_{1-8}$	−0.007	−0.007	0.058	−0.172	0.129
$4D_{1-8}$	0.015	0.015	0.092	−0.173	0.050

4. Conclusion

The one- and two-photon absorption spectra, TPA transitions and TPA cross-sections of the studied compounds have been explored in detail using DFT, ZINDO and FTRNLO programs. The results obtained allow us to conclude that OPA wavelength maxima $\lambda^{(1)}_{max}$s of the designed molecules with D or A substituents have red-shifts compared with molecule SII. And δ_{max} values increase with increasing the number of D/A pair. The δ_{max} values of D–A type are close to one of A–A, and larger than that of D–D and SII molecules. The molecules show larger δ_{max} when electron donor and acceptor locate on the opposite site, which is ascribed to the enhancement of the ICT between D and A. It is further confirmed that macrocyclic thiophenes with stronger D/A substitution have larger δ_{max}. In addition, the distributions of electron clouds have been interpreted by the values of ΔQ_1 and ΔQ_2. Moreover, δ_{max} of all studied molecules can be rudely predicted by the three-state approximation. While M_{0k} and M_{kn} in these macrocycles play important roles on δ_{max}. Besides, $f_{0k} \times f_{kn}$ is in direct proportion to δ_{max}. In summary, the present computational results provide a useful guideline for the design of novel D–π–A molecules with large TPA cross-section by enlarging the strength, increasing the number and changing the position of electron donor and acceptor substituents based on the circular π-conjugated skeleton. All above suggest this series of macrocyclic thiophene-based derivatives are expected to be promising two-photon absorption materials.

Acknowledgement

This work is supported by the Natural Science Foundation of China (No. 20973078 and 20673045), special funding to basic scientific research projects for Central Colleges, as well as the Open Project of the State Key Laboratory for Superamolecular Structure and Material of Jilin University (SKLSSM200716).

References

[1] Kanis DR, Ratner MA, Marks TJ. Design and construction of molecular assemblies with large second-order optical nonlinearities. Quant Chem Aspect Chem Rev 1994;94:195–242.
[2] Boni LD, Andrade AA, Corrêa DS, Balogh DT, Zilio SC, Misoguti L, et al. Nonlinear absorption spectrum in MEH-PPV/chloroform solution: a competition between two-photon and saturated absorption processes. J Phys Chem B 2004;108:5221–4.
[3] Margineanu A, Hofkens J, Cotlet M, Habuchi S, Stefan A, Qu JQ, et al. Photophysics of a water-soluble rylene dye: comparison with other fluorescent molecules for biological applications. J Phys Chem B 2004;108:12242–51.
[4] Göeppert-Mayer M. Über elementaraktemit zwei quantensprungen. Ann Phys 1931;9:273–95.
[5] Maruo S, Nakamura O, Kawata S. Three-dimensional microfabrication with two-photon-absorbed photopolymerization. Opt Lett 1997;22:132–4.

[6] Pham TA, Kim DP, Lim TW, Park SH, Yang DY, Lee KS. Three-dimensional SiCN ceramic microstructures via nano-stereolithography of inorganic polymer photoresists. Adv Funct Mater 2006;16:1235–41.
[7] Lin TC, He GS, Zheng Q, Prasad PN. Degenerate two-/three-photon absorption and optical power-limiting properties in femtosecond regime of a multi-branched chromophore. J Mater Chem 2006;16:2490–8.
[8] Parthenopoulos DA, Rentzepis PM. Three-dimensional optical storage memory. Science 1989;245:843–5.
[9] Larson DR, Zipfel WR, Williams RM, Clark SW, Bruchez MP, Wise FW, et al. Water-soluble quantum dots for multiphoton fluorescence imaging in vivo. Science 2003;300:1434–6.
[10] Kim HM, An MJ, Hong JH, Jeong BH, Kwon O, Hyon JY, et al. Two-photon fluorescent probes for acidic vesicles in live cells and tissue. Angew Chem Int Ed 2008;47:2231–4.
[11] Kim OK, Fort A, Barzoukas M, Blanchard-Desce M, Lehn JM. Nonlinear optical chromophores containing dithienothiophene as a new type of electron relay. J Mater Chem 1999;9:2227–32.
[12] Würthner F, Effenberger F, Wortmann R, Krämer P. Second-order polarizability of donor-acceptor substituted oligothiophenes: substituent variation and conjugation length dependence. Chem Phys 1993;173:305–14.
[13] Bednarz M, Reineker P, Mena-Osteritz E, Baeuerle P. Optical absorption spectra of linear and cyclic thiophenes–selection rules manifestation. J Lumin 2004;110:225–31.
[14] Leng WN, Bazan GC, Kelley AM. Solvent effects on resonance Raman and hyper-Raman scatterings for a centrosymmetric distyrylbenzene and relationship to two-photon absorption. J Chem Phys 2009;130:044501.
[15] Bhaskar A, Ramakrishna G, Hagedorn K, Varnavski O, Osteritz EM, Ba1uerle P, et al. Enhancement of two-photon absorption cross-section in macrocyclic thiophenes with cavities in the nanometer regime. J Phys Chem B 2007;111:946–54.
[16] Casado J, Zgierski MZ, Fuhrmann G, Juan PB, Navarreteb JTL. Structural implications of ring shape, dimension, and metal atom insertion in nanosized cyclic oligothiophenes: joint Raman and density functional theory study. J Chem Phys 2006;125:044518.
[17] Fuhrmann GL. Synthesis and characterization of oligothiophene-based fully π-conjugated macrocycles the department of organic chemistry II. Germany: University of Ulm; 2006.
[18] Huang S, Ren AM, Zou LY, Zhao Y, Guo JF, Feng JK. Computational study of the one- and two-photon absorption properties of macrocyclic thiophene derivatives. Dyes Pigments 2011;91:248–57.
[19] Huang S, Ren AM, Zou LY, Zhao Y, Guo JF, Feng JK. Computational study of the electronic structures, UV–Vis spectra and static second-order nonlinear optical susceptibilities of macrocyclic thiophene derivatives. J Mol Model, doi:10.1007/s00894-011-1082-8.
[20] Zhou X, Ren AM, Feng JK, Liu XJ. Theoretical study of two-photon absorption properties of a series of double-layer paracyclophane derivatives. J Phys Chem A 2003;107:1850–8.
[21] Zhao Y, Truhlar DG. Hybrid meta density functional theory methods for thermochemistry, thermochemical kinetics, and noncovalent interactions: the MPWB95 and MPWB1K models and comparative assessments for hydrogen bonding and van der Waals Interactions. J Phys Chem A 2004;108:6908–18.
[22] Zhao Y, Truhlar DG. Benchmark databases for nonbonded interactions and their use to test density functional theory. J Chem Theory Comput 2005;1:415–32.
[23] Frisch MJ, Trucks GW, Schlegel HB, Scuseria GE, Robb MA, Cheeseman JR, et al. Gaussian 03 (revision D02). Pittsburgh, PA: Gaussian Inc.; 2003.
[24] Anderson WP, Edwards WD, Zerner MC. Calculated spectra of hydrated ions of the first transition-metal series. Inorg Chem 1986;25:2728–32.
[25] Zhao Y, Ren AM, Feng JK, Zhou X, Ai XC, Su WJ. Theoretical study of solvent effect on one- and two-photon absorption properties of starburst DCM derivatives. Phys Chem Chem Phys 2009;11:11538–45.
[26] Kogej T, Beljonne D, Meyers F, Perry JW, Marder SR, Brédas JL. Mechanisms for enhancement of two-photon absorption in donor–acceptor conjugated chromophores. Chem Phys Lett 1998;298:1–6.
[27] Orr BJ, Ward JF. Perturbation theory of the non-linear optical polarization of an isolated system. Mol Phys 1971;20:513–26.
[28] Bishop DM, Luis JM, Kirtman B. Vibration and two-photon absorption. J Chem Phys 2002;116:9729–39.
[29] Beljonne D, Wenseleers W, Zojer E, Shuai Z, Vogel H, Pond SJK, et al. Role of dimensionality on the two-photon absorption response of conjugated molecules: the case of octupolar compounds. Adv Funct Mater 2002;12:631–41.
[30] Fuhrmann G, Debaerdemaeker T, Bäuerle P. C–C bond formation through oxidatively induced elimination of platinum complexes – a novel approach towards conjugated macrocycles. Chem Commun; 2003:948–9.
[31] Kromer J, Rios-Carreras I, Fuhrmann G, Musch C, Wunderlin M, Debaerdemaeker T, et al. Synthesis of the first fully alpha-conjugated macrocyclic oligothiophenes Cyclo[n]thiophenes with tunable cavities in the nanometer regime. Ang Chem Int Ed 2000;39:3481–6.
[32] Hilderbrand SA, Weissleder R. Near-infrared fluorescence: application to in vivo molecular imaging. Curr Opin Chem Biol 2010;14:71–9.